Supplementary Information

Amphiphilic Distyrylbenzene Derivatives as Potential Therapeutic and Imaging Agents for the Soluble and Insoluble Amyloid β Aggregates in Alzheimer's Disease

Liang Sun,[1] Hong-Jun Cho,[1] Soumyo Sen,[3] Andres S. Arango,[3] Truc T. Huynh,[4,5] Yiran Huang,[1] Nilantha Bandara,[4] Buck E. Rogers,[4] Emad Tajkhorshid,[3] and Liviu M. Mirica[1,2,*]

[1] Department of Chemistry, Beckman Institute for Advanced Science and Technology, The Neuroscience Program, University of Illinois at Urbana-Champaign, 600 S. Mathews Avenue, Urbana, Illinois 61801, United States

[2] Hope Center for Neurological Disorders, Washington University School of Medicine, St. Louis, MO 63110, United States

[3] NIH Center for Macromolecular Modeling and Bioinformatics, Beckman Institute for Advanced Science and Technology, Center for Biophysics and Quantitative Biology and Department of Biochemistry, University of Illinois at Urbana-Champaign, Urbana, IL 61801, United States

[4] Department of Radiation Oncology, Washington University School of Medicine, St. Louis, Missouri 63108, United States

[5] Department of Chemistry, Washington University, St. Louis, Missouri 63130, United States

* e-mail: mirica@illinois.edu

Table of Contents

Experimental Details

General Methods

All reagents were purchased from commercial sources and used as received unless stated otherwise. All solutions and buffers were prepared using metal-free Millipore water that was treated with Chelex resin overnight and filtered through a 0.22 μm nylon filter. ^{1}H (300.121 MHz) NMR spectra were recorded on a Varian Mercury-300 spectrometer. Chemical shifts were reported in ppm downfield from tetramethylsilane. UV−visible spectra were recorded on a Varian Cary 50 Bio spectrophotometer and were reported as λ_{max}, nm (ε, M^{-1} cm^{-1}). 5xFAD transgenic mice (Tg6799 line) overexpressing mutant human APP (695) with the Swedish (K670N, M671L), Florida (I716V), and London (V717I) were purchased from Jackson Laboratories (Bar Harbor, ME, USA). TEM analysis was performed at the Nano Research Facility (NRF) at Washington University. All normal and C-18 reversed-phase column chromatography was performed on a Teledyne Isco Combiflash Rf+.

Synthetic Details

Synthesis of 1. Compound **1** was synthesized according to the previously reported procedure.[1] A mixture of 1-bromo-4-(4-nitrostyryl)benzene (304 mg, 1 mmol) and $SnCl_2$ (948 mg, 5 mmol) in anhydrous ethanol (30ml) was refluxed overnight under nitrogen. The solution was allowed to cool and then neutralized by addition of saturated $NaHCO_3$ solution followed by extraction with ethyl acetate (3×20 mL). The organic layer was washed with brine twice and then dried over magnesium

sulfate. Evaporation of the solvent provided the product as compound **1** (205 mg, 75%), which was used without further purification in the next step.

Synthesis of 2. Compound **2** was synthesized according to the previously reported procedure. [2] To a mixture of compound **1** (274 mg, 1 mmol), paraformaldehyde (300 mg, 10 mmol), and sodium cyanoborohydride (189 mg, 3 mmol) was added into acetic acid (20 ml). The reaction was stirred at room-temperature overnight and then poured into 50 ml water. The resulting solution was basified to pH 8-9 with sodium carbonate and then extracted with dichloromethane (3×20 mL). The organic layer was washed with brine twice and then dried over magnesium sulfate. The solvent was removed under vacuum, and the residue was recrystallized by DCM/hexane to yield a yellow solid (181 mg, 60%), which was used without further purification in the next step.

Synthesis of Pre-LS-4. A mixture of 2-methoxy-4-vinylphenol (200 mg, 1.3 mmol), compound **2** (393 mg, 1.3 mmol), triethanolamine (10 ml) and $Pd(OAc)_2$ (23 mg, 0.1 mmol) was stirred under nitrogen at 100 °C for 24 h. The reaction was cooled to room temperature, quenched with water (5 ml), and used acetone to dissolve the residue which followed by vacuum filtration to remove the palladium black. After the solvents evaporated, the crude product was recrystallized by ethyl acetate to yield a yellow pure product (290 mg, 60%). ^{1}H NMR (DMSO-d6): δ (ppm): 9.13 (s, 1H), 7.49 (s, 4H), 7.41 (d, 2H, J = 8.4Hz), 7.19 (s, 1H), 7.12 (d, 2H, J = 16.4 Hz), 7.04 (d, 1H, J = 16.4 Hz), 7.00-6.90 (m, 2H), 6.75 (d, 1H, J = 8.1 Hz), 6.70 (d, 2H, J = 8.5 Hz), 3.82 (s, 3H), 2.91 (s, 6H). ^{13}C NMR δ (ppm): 150.42, 148.31, 147.12, 137.11, 136.40, 129.28, 128.84, 128.61, 127.98, 126.81, 126.63, 125.60, 125.51, 123.75, 120.61, 116.05, 112.73, 110.24, 56.08, 40.44, Calcd for $[M + H]^+$: m/z 372.1964. Found m/z 372.1966.

Synthesis of LS-4. Paraformaldehyde (3 mg, 0.1 mmol) was added to a solution of 1,4-dimethyl-1,4,7-triazacyclononane (9 mg, 0.05 mmol) in MeCN (10 mL), and the resulting mixture was

heated to reflux for 30 min. A solution of compound Pre-LS-4 (20 mg, 0.05 mmol) in MeCN (10 mL) was added to the reaction flask, and the solution was refluxed for an additional 24 h. The solvent was removed, and the resulting residue was purified by C-18 reversed-phase column using MeCN/H_2O/TFA (gradient wash from 10:90:1 to 40:60:1) to yield a yellow solution. The solution was neutralized by saturated $NaHCO_3$ solution (30 mL) and extracted by dichloromethane (3×10 mL). The solvent was removed to yield a yellow solid (8 mg, yield 30%). ^{1}H NMR ($CDCl_3$): δ (ppm): 7.45 (s, 4H), 7.42 (d, 2H, J = 8.8 Hz), 7.06 (d, 1H, J = 16.4 Hz), 7.01 (d, 1H, J = 1.8 Hz), 6.98 (s, 1H), 6.92 (d, 1H, J = 16.3 Hz), 6.90 (d, 1H, J = 16.3 Hz), 6.83 (s, 1H), 6.72 (d, 2H, J = 8.8 Hz), 3.95 (s, 3H), 3.86 (s, 2H), 2.99 (s, 6H), 2.97 – 2.91 (m, 4H), 2.88 – 2.81 (m, 4H), 2.48 (s, 4H), 2.01 (s, 6H). ^{13}C NMR δ (ppm): 152.80, 150.89, 139.79, 138.84, 131.18, 130.93, 130.79, 130.23, 129.09, 128.95, 128.52, 128.40, 126.73, 125.74, 122.57, 115.14, 111.24, 63.21, 60.26, 58.65, 55.91, 48.95, 43.12. ESI-MS. Calcd for $[M + H]^+$: m/z 541.3543. Found m/z 541.3549.

Amyloid β Peptide Experiments

$A\beta_{42}$ powder was prepared by dissolving commercial $A\beta_{42}$ peptide (AnaSpec or GLbiochem) in ammonium hydroxide solution (1%, v/v). The solution was then aliquoted out and lyophilized overnight. The resulting aliquoted powder was stored at –80 °C. $A\beta_{42}$ monomers were generated by dissolving $A\beta_{42}$ powder in 1,1,1,3,3,3-hexafluoro-2-propanol (HFIP, 1 mM) and incubating for 1 h at room temperature. The solution was then evaporated overnight and dried by vacuum centrifuge to result in monomeric films. $A\beta_{42}$ fibrils were generated by dissolving the monomeric $A\beta_{42}$ films in DMSO, diluting into the appropriate buffer, and incubating for 24 h at 37 °C with continuous agitation (final DMSO concentration was < 2%). For preparation of $A\beta_{42}$ oligomers, the peptides were suspended in PBS buffer and incubated overnight at 4 °C.

Fluorescence Spectroscopy

All fluorescence measurements were performed by using a SpectraMax M2e plate reader (Molecular Devices). The fluorescence spectra of Pre-LS-4 and LS-4 solution (100 μL PBS, 5.0 μM) were recorded with excitation at 380 nm and emission wavelength from 400 to 680 nm. To PBS solutions (100 μL) of compounds Pre-LS-4 and LS-4 (5.0 μM), various $A\beta_{42}$ species were added to the solution, final concentrations of 5.0 μM, 25.0 μM, and their fluorescence spectra (λ_{max} of emission) were determined as described as above.

Time-dependent $A\beta_{42}$ Fibrils Formation

For monitoring the formation of $A\beta_{42}$ fibrils, a peptide solution of 100 μM $A\beta_{42}$ was prepared as above and incubated at 37 °C with shaking for 48 hours, in the presence of 5 μM ThT. Fluorescence intensities were recorded at selected time points by mixing 25 μM peptide and 5 μM LS-4 or Pre-LS-4 solution. The ThT fluorescent signal was monitored at 485 nm upon 435 nm excitation. Pre-LS-4 was excited at 360 nm and the emission was recorded at 470 nm. LS-4 and Cu^{2+}-LS-4 were excited at 380 nm, and the emission was recorded at 470 nm.

Trolox Equivalent Antioxidant Capacity (TEAC) Assay

The antioxidant ability of compounds was investigated by TEAC assay with the established protocol.[3] ABTS (8.2 mg, 2,7 eq.) and $K_2S_2O_8$ (1.6 mg, 1 eq.) were dissolved in 2 mL de-ionized

water to prepare $ABTS^{+\bullet}$ cation radicals. The reaction was allowed to occur overnight in the dark at room temperature. The $ABTS^{+\bullet}$ solution was and aliquoted (3-42 μL) into a transparent 96-well plate and diluted with methanol to 300 μL; each volume was monitored at 740 nm via UV-vis spectroscopy to determine the concentration of the radical solution displaying an absorbance around 0.7. The absorbance of the $ABTS^{+\bullet}$ radicals increased linearly in this range and a volume of 36 μL was selected for the following TEAC assay giving an absorbance approximately 0.7. Trolox, glutathione, Pre-LS-4 and LS-4 were dissolved in methanol to prepare 1.5 mM stock solution. Each solution in different final concentrations (25, 50, 75 ,100 μM) were added into 96-well plate and diluted with methanol to a volume of 270 μL. After adding 36 μL ABTS solution into each well, the absorbance at 740 nm was recorded at different time points (1, 3, 6, 15 min) immediately.

Cu^{2+}-Induced Ascorbate Consumption Assay

A 10 mM stock solution of ascorbate was prepared in 10 mM PBS buffer, and a 10 mM stock solution of $CuSO_4$ was prepared in Millipore water. For both Pre-LS-4 and LS-4, the 5 mM stock solution was prepared in DMSO. Monomeric $A\beta_{42}$ was dissolved in PBS buffer to make a 100 μM stock solution. Final concentrations in the assay were as follows: 100 μM ascorbate, 10 μM $CuSO_4$, 12 μM $A\beta_{42}$, 24 μM compounds. For the assay without the Aβ peptide, three spectra were collected as a function of time as follows: 1) Ascorbate was first added into the PBS buffer following the addition of $CuSO_4$ solution; 2) The 24 μM compounds were premixed with $CuSO_4$ solution for 30 min following introducing the Cu-complex solution to the 100 μM ascorbate solution; 3) Ascorbate was first added into the PBS buffer following the addition of $CuSO_4$ solution, when the absorbance at 265 nm reached half of that at the starting point, the prepared 24 μM compounds were added to

the solution. The solution was monitored at 265 nm for 40 min to collect the time-dependent spectra. Similar conditions were used for the assay with the presence of Aβ.

Cytotoxicity Studies (Alamar Blue Assay)

Mouse neuroblastoma Neuro2A (N2A) cell lines were purchased from the American Type Culture Collection (ATCC). Cells were grown in DMEM/10% FBS, which is the regular growth media for N2A cells, in a humidified atmosphere with 5% CO_2 at 37 °C. N2A cells were seeded in a 96-well plate (2.5×10^4/well) with DMEM/10% FBS. The media was changed to DMEM/N-2 media 24 h later. After 1 h, the reagents (20 μM $A\beta_{42}$ species, 5 μM compounds, and 20 μM $CuCl_2$) were added. Owing to the poor solubility of compounds in the media, the final amount of DMSO used was 1% (v/v). After an additional incubation of 40 h, the Alamar Blue solution was added in each well and the cells were incubated for 90 min at 37 °C. Fluorescence intensity was measured at 590 nm (excitation wavelength = 560 nm).

Histological Staining of 5xFAD Mice Brain Sections

To evaluate the Aβ binding specificity of the compounds and Cu complexes *in vitro*, brain sections from 7-month old 5xFAD mice were washed with PBS (3 × 5 min) and blocked with bovine serum albumin (2% BSA in PBS, pH 7.4, 10 min). Then the sections were incubated with 25 μM Pre-LS-4, LS-4 or their Cu-complexes, and sequentially stained with 5 μM Congo Red, HJ3.4 antibody (Professor David Holtzman, 1 μg/ml) or amyloid beta oligomer-specific monoclonal antibody (Agrisera, 5 μg/ml) solution for 1 h respectively. The brain sections were treated with 2%BSA-PBS again for 4 min to remove any compounds or antibodies that were non-specifically binding

to the tissue. Finally, the sections were washed with PBS (3 × 2 min), DI water (2 min) and mounted with non-fluorescent mounting media (Vectashield). To confirm the *in vivo* Aβ binding specificity of LS-4, the brain sections from LS-4 treated 5xFAD mice were directly incubated with Congo Red, HJ3.4 antibody and amyloid beta oligomer-specific monoclonal antibody, followed by the same incubation and wash steps for in vitro brain sections staining. For Iba1 and AT-8 antibody staining, the antigen retrieval was performed by pretreating the brain sections with citrate buffer (10 mM sodium citrate, 0.05% tween 20, pH 6.0) for 30 minutes at 80°C. After epitope retrieving, the brain sections were permeabilized in 0.25% triton-x100-PBS for 30 minutes at room temperature and washed with PBS buffer (3 × 5 min).Then, the brain sections were incubated with ThS solution for 30 minutes, and treated with the blocking solution (0.1% triton-x100, 0.2% dry milk, and 1% BSA in PBS) at room temperature for 1 h, and incubated with Iba1 and AT-8 antibodies (1 μg/ml) overnight at 4°C. After incubation, the brain sections were washed by PBS (3 × 2 min) and mounted with mounting media on the slides. The primary antibodies were labeled with dye CF594 via Mix-n-Stain™ CF™ 594 Antibody Labeling Kit (Sigma Aldrich). The stained brain sections were observed by using EVOS FL Auto 2. The maximum intensity projection images of the CF594-Iba1- and CF594-AT8-stained brain sections were obtained from 30 Z-sections collected at 1 μm intervals. The number and fluorescence intensity of amyloid plaques, microglia cells, and aggregated p-tau in each brain section were quantitatively analyzed by the ImageJ program under the same minimum and maximum values of fluorescence intensity. Colocalization analysis and determination of the Pearson's correlation coefficient was performed with the imaging software Fiji (ImageJ 1.52p).

Log D Measurements

The determination of log D values for Pre-LS-4 and LS-4 was performed by using a slightly modified reported procedure.[4] Solutions of Pre-LS-4 and LS-4 (final concentration 25 μM) were added to the premixed suspension containing 0.5 ml octanol and 0.5 ml octanol-saturated PBS buffer (pH 7.4). The resulting mixture was stirred vigorously for 5 minutes and centrifuged 2000 rpm for 5 minutes. The octanol layer was separated from the aqueous layer, and the fluorescence spectrum was recorded. To the 0.5 ml aqueous layer, 0.5 ml of PBS-saturated octanol was added, the mixture was shaken vigorously for 5 minutes, centrifuged, and then the octanol layer was separated. The fluorescence spectrum of the second octanol layer was recorded, and the log D value was calculated as the fluorescence intensity ratio for the two octanol layers. Each experiment was completed in triplicate and the errors represent standard deviations for the average logD values.

To confirm the protonation states of LS-4 under physiological pH, the pK_a values of LS-4 were predicted by using Schrödinger Suite. The pH range was set as 7.0 ± 2.0 and the pK_a values were predicted using Epik, to give the values of 10.02, 8.49, 5.88, and 5.26, which were assigned to protonation sites corresponding to the phenol group for the 10.02 value, the three amine groups of the triazamacrocycle for the 8.49 and 5.88 values, and the dimethylamino group for the 5.26 value, respectively. Based on these pK_a values, compound LS-4 should be mono-protonated at pH 7.4, with the N atoms of the triazamacrocyle interacting with the proton, and similar to what was reported previously for a related compound.[5]

Animal Studies

Experiments involving animals were performed in compliance with the Institutional Animal Care and Use committee of the University of Illinois at Urbana-Champaign. Three-month old 5xFAD

mice were divided into two groups. The two groups of 6 mice each were treated daily with a freshly prepared solution of LS-4 (1 mg/kg of body weight in 200 μL of PBS, pH 7.4, 1% DMSO) or vehicle (200 μL of PBS, pH 7.4, 1% DMSO) via intraperitoneal injection. After 10 or 30 days, all mice were sacrificed under deep anesthesia for perfusion and brain harvesting.

Quantification of $A\beta_{40}$ & $A\beta_{42}$ in AD Mouse Brain Sections

The frozen brain sections (half hemisphere) was weighed and homogenized in cold PBS (100 mg/ml) with a protease inhibitor cocktail (1: 100 dilution, Thermo Fisher Scientific). The supernatant containing soluble Aβ species was collected by centrifuging at 16000 × g for 20 min at 4 °C. The resulting pellet was resuspended in 5 M guanidine HCl/50 mM Tris-HCl (pH 8, 100 mg/mL, 10% w/v) and incubated at room temperature for 4 h. The supernatant containing insoluble Aβ species was collected by centrifuging at 16000 × g for 20 min at 4 °C. Both supernatants were diluted 1000-10000 folds, and then the amounts of soluble and insoluble Aβ species were determined using the human $A\beta_{40}$&$A\beta_{42}$ ELISA kits. (Invitrogen)

Aβ Fibril Modeling

We created a periodic Aβ fibril starting from an NMR resolved 2×6-mer fibril structure having a two-fold symmetry with respect to the fibril axis (PDB ID: 2LMN),[6] while taking into account the natural twist of the fibril as reported in a recent cryoEM structure.[7] A two-fold symmetric Aβ peptide pair of the NMR structure was used as a building block in the preparation of the periodic fibril. Our final fibril model consisted of a total of 180 peptide pairs with a spacing between adjacent pairs along the fibril axis of 4.8 Å, and a twist angle of 1º in the plane normal to the fibril

axis. The modeled periodic fibril was simulated in an explicit water box for a 10-ns equilibration run followed by a 100-ns production run. The reason to use 2LMN instead of other PDB structures was based on our need to replicate the PDB structure linearly in space to generate a structure representing the fibril. The other available structures are not long enough to differentiate between ligand binding at the edge of the fibril, and binding in the middle of the fibril by fully inserting into the fibril cavity. Simulation of other shorter structures exhibited clear instability (shearing between the monomers), likely due to the fact that only a portion of the fibril is resolved/reported in the PDBs. Finally, we expect similar modes of binding for LS-4 and Pre-LS-4 for fibril structures generated by other available structures.

Ensemble Molecular Docking of LS-4 and Pre-LS-4 onto the Aβ Fibril

To characterize LS-4 and Pre-LS-4 binding to the Aβ fibril, ensemble molecular docking was performed. We used 100 snapshots of a segment (comprised of 24 peptide pairs) of the periodic fibril taken from 100-ns production run of the full periodic fibril simulation in our ensemble docking by Auto Dock Vina.[8] For docking, a grid box of size 100Å × 80Å ×140Å was used and positioned at the center of the fibril. Both compounds were docked onto each snapshot with an exhaustiveness of 40, with 10 poses collected for each snapshot, yielding a total of 1,000 docked poses for each compound. For LS-4, in 60-65% of the poses, the compound is partly inserted into the Aβ fibril cavity where the planar portion of the compound is fully inserted and the cage hangs outside the fibril, whereas only in 5% of the poses it is fully inserted into the cavity (Figure S15a). We identified an LS-4 pose out of the 60-65% partially inserted poses with the strongest docking score for the MD simulations. In the case of Pre-LS-4, the compound is fully inserted into the fibril

cavity in almost 85% of the poses (Figure S15b) and the pose corresponding to the strongest docking score was selected for the MD simulations.

Ensemble Molecular Docking of LS-4 and Pre-LS-4 onto the Aβ Oligomer

To probe the molecular interactions of LS-4 and Pre-LS-4 with the Aβ oligomer, ensemble molecular docking was employed. Three prior 500-ns simulations of membrane-bound $A\beta_{42}$ octamers, as described in Ciudad et. al.,[9] were used to obtain the snapshots needed for docking. Trajectory snapshots of only the Aβ oligomer were extracted every 100 ps, yielding a total of 15,000 oligomeric Aβ snapshots. Next a docking grid box of (54Å × 54Å × 100Å) was used to envelop the entire Aβ octamer oligomer. As with the fibril studies, Auto Dock Vina was used for docking in the selected grid box following a similar protocol, yielding 10 poses per snapshot for a total of 300,000 docked poses, 150,000 for each compound (Figure S16). The resultant poses were then filtered by docking score, with the poses having the most favorable docking scores selected for further simulations. The selected compound-oligomer poses recombined with their original corresponding membrane coordinates from the seed trajectory used to extract snapshots, to preserve membrane morphology prior to MD simulation runs.

Molecular Dynamics (MD) Simulations

A total of 4 MD simulation systems were prepared in an explicit water box, where 2 systems corresponded to both compounds (LS-4 and Pre-LS-4) docked to Aβ fibril and the remaining 2 systems corresponded to the same compounds docked to the Aβ oligomers. In the case of the compound-Aβ fibril complex, both systems (LS-4 partially inserted into the Aβ fibril, and Pre-LS-

4 fully inserted into the Aβ fibril, respectively) were solvated in 150 mM NaCl solution. In the case of compound-Aβ oligomer complex, both complexes (LS-4-Aβ oligomer and Pre-LS-4-Aβ oligomer, respectively) were embedded in the lipid bilayer corresponding to the coordinates of the simulation trajectory snapshot used for ensemble molecular docking, and then were solvated and ionized (150 mM NaCl) using the CHARMM-GUI webserver as described in Ciudad et. al. [9] All the simulations corresponding to compounds docked into Aβ fibril and Aβ oligomer were performed for 100 ns by NAMD3[10,11] molecular dynamics package using CHARMM36m[12,13] force field for the protein and lipids, and the CHARMM General Force Field for the compounds.[14] The TIP3P[15] water model was utilized for explicit water solvation. The systems were simulated using an NPT ensemble with a 1.0 atm pressure, 310 K temperature, and a time step of 2 fs. Moreover, constant pressure was maintained using the Nose–Hoover Langevin piston method.[16] The constant temperature was maintained using Langevin dynamics with a damping coefficient of 0.5 ps^{-1}. A 12 Å cutoff was used for nonbonded interactions with a smoothing function implemented after 10 Å. The bond distances of the hydrogen atoms were constrained using the SHAKE algorithm.[17] For long-range electrostatic calculations, the particle mesh Ewald (PME)[18] method was used, with a grid density of < $1Å^{-3}$. Visualization of the simulations was performed using Visual Molecular Dynamics (VMD).

Trajectory Analysis

The MD trajectories were analyzed using VMD and its plugins.[19] The interactions energy between compounds and protein was calculated using NAMD Energy plugin of VMD. In the case of membrane bound oligomers, interaction energies between compounds and protein-lipid complex were calculated using the same tool. In the calculation, the dielectric constant for electrostatic

interaction energy was considered to be 1.0. All the analyses were performed for the last 25 ns of the simulations.

Radiolabeling

^{64}Cu ($t_{1/2}$ = 12.7 hours; β^+, 0.653 MeV [17.8 %]) was produced by a (p, n) reaction on enriched ^{64}Ni on a TR-19 biomedical cyclotron (Advanced Cyclotron Systems Inc, British Columbia, Canada) at Mallinckrodt Institute of Radiology, Washington University School of Medicine, and purified with an automated system by using standard procedures.[20] A stock solution of $^{64}CuCl_2$ was diluted with a 10-fold excess of 0.1 M ammonium acetate (NH_4OAc), pH 5.5 for radiolabelling. Labelling of BFCs with ^{64}Cu was achieved by adding 100 µL of a 1 mM LS-4 solution to 37 MBq (1 mCi) of $^{64}CuCl_2$ in 100 µL of 0.1 M NH_4OAc, pH 5.5. The reactions were incubated on a thermomixer with 800 rpm agitation at 45 °C for 20 - 60 min. Radiolabelled complexes were analysed by using high-performance liquid chromatography (HPLC, Shimadzu 10Avp system), with a mobile phase of water (0.1% TFA) and acetonitrile (0.1% TFA), 0-100% acetonitrile over 10 min with a 1 mL/min flow rate. A radiochemical yield of greater than 95% was achieved for all labelled compounds and, therefore, they were used without further purification.

Lipophilicity Studies

The ^{64}Cu-LS-4 complex (5 µL, 0.37 MBq, 10 µCi) were added into a 1:1 v/v mixture of n-octanol and PBS (500 µL/ea). The samples were vortexed at 1,000 rpm for 1 h, and the layers were then allowed to separate for 30 min. Aliquots (100 µL) from the aqueous and the *n*-octanol layers were removed and counted separately in an automated gamma counter. The partition coefficients were

calculated by using the ratio of (activity detected in n-octanol)/ (activity detected in PBS layer) to get the log D values. The experiment was conducted in triplicate of triplicates, and the overall average was recorded as the final log D value for each compound.

Ex vivo Autoradiography Studies

Brain sections of 10-month old 5xFAD transgenic mice and aged-matched WT mice were obtained as described previously[21] and immersed into a cryo-protectant solution. These sections were sorted and washed with 100% PBS three times. The sections were placed in a 12-well plate (1 brain section per well) and ~0.925 MBq (25 μCi) of ^{64}Cu-LS-4 in a 1 mL total volume was added to cover completely the brain section and incubated for 1 h at room temperature in a shielded bunker. For the blocking studies, the non-radioactive Aβ-binding compound 4-hydroxyphenylbenzothiazole shown below was used to treat first the brain sections prior to the addition of the radioactive solutions. After the incubation, brain sections were washed by using PBS with five 1-min cycles, mounted on a microscope glass slide and briefly air-dried. The imaging slides were mounted on a phosphor imaging screen plate (GE Healthcare Life Sciences) and were exposed overnight at -20 ºC. The plates were scanned using biomolecule imager (Typhoon FLA 9500, GE) and the resulting images were processed using the ImageJ (v1.48, public domain) software.

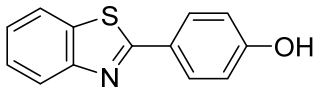

2-(4-hydroxyphenyl)benzothiazole (B1)

Biodistribution Studies

All animal experiments were performed in compliance with the Guidelines for Care and Use of Research Animals established by the Division of Comparative Medicine and the Animal Studies Committee of Washington University School of Medicine. Biodistribution studies were conducted in 10-month old 5xFAD transgenic mice and age-matched wild type mice**.** The injection dose was prepared by diluting it in a 90 % saline solution. The uptake of ^{64}Cu-LS-4 was evaluated in mice that were injected via the tail vein with 0.22-0.37 MBq (6-10 μCi) of ^{64}Cu-LS-4 in 100 μL saline solution per animal. After each time point (2, 60, and 240 min), mice were anesthetized with 1-2% isoflurane and euthanized by cervical dislocation. Brain, blood, kidney, liver, and other organs of interest were harvested, and the amount of radioactivity in each organ was counted on a gamma counter containing a NaI crystal. The data were corrected for radioactive decay, and percent injected dose per gram (%ID/g) of tissue was calculated. All samples were calibrated against a known standard. Quantitative data were processed by Prism 6 (GraphPad Software, v 6.03, La Jolla, CA) and expressed as Mean ± SD. Statistical analysis was performed by using one-way analysis of variance. Differences at the 95% confidence level ($p < 0.05$) were considered statistically significant.

Supplementary Figures

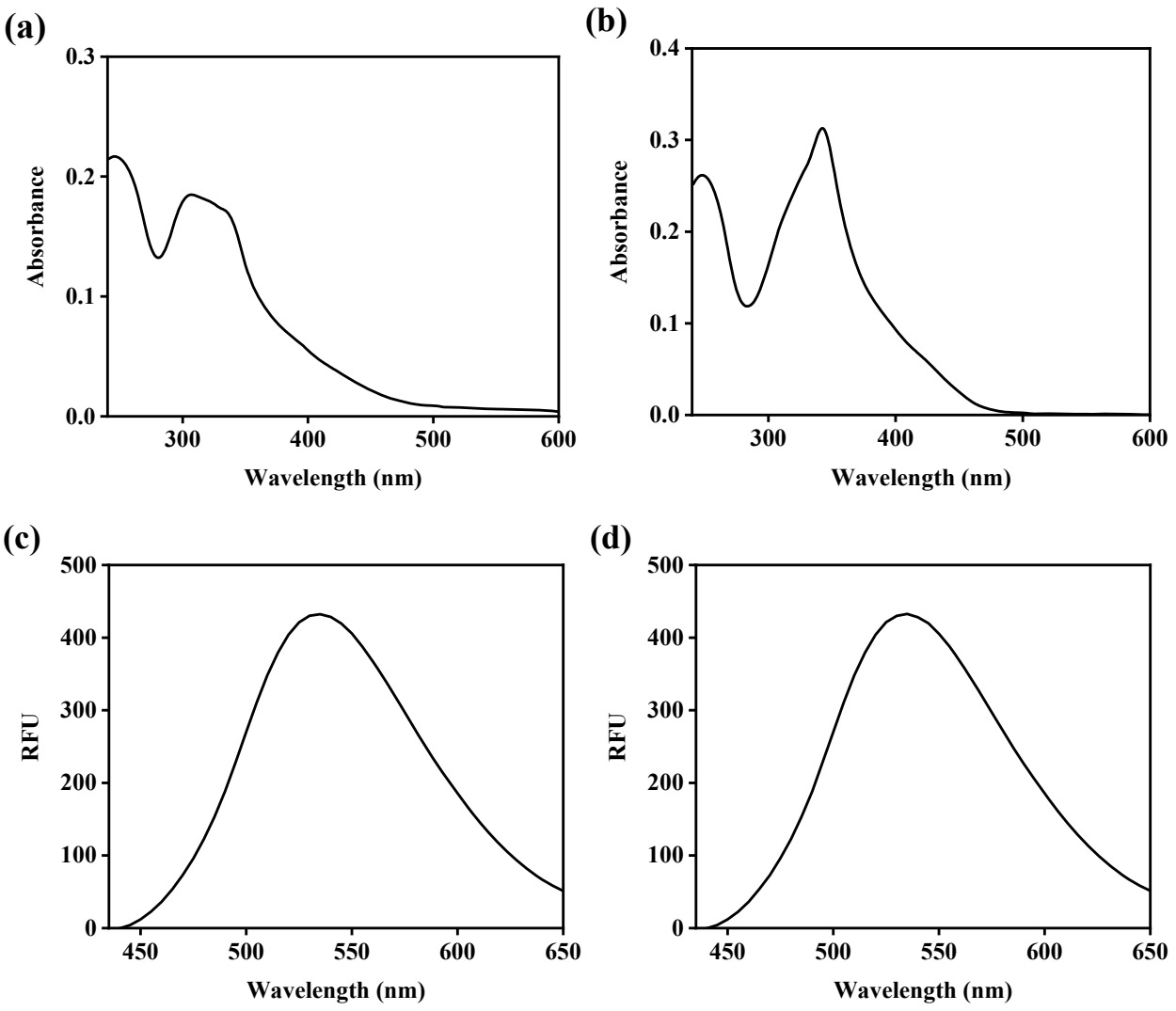

Figure S1. Optical properties of compound Pre-LS-4 and LS-4. (a) UV-Vis spectrum of Pre-LS-4 (25 μM in PBS, pH 7.4); (b) UV-Vis spectrum of LS-4 (25 μM in PBS, pH 7.4); (c) Fluorescence emission spectrum of Pre-LS-4 (25 μM in PBS, pH 7.4), obtained under excitation at 380 nm. (d) Fluorescence emission spectrum of LS-4 (25 μM in PBS, pH 7.4), obtained under excitation at 380 nm.

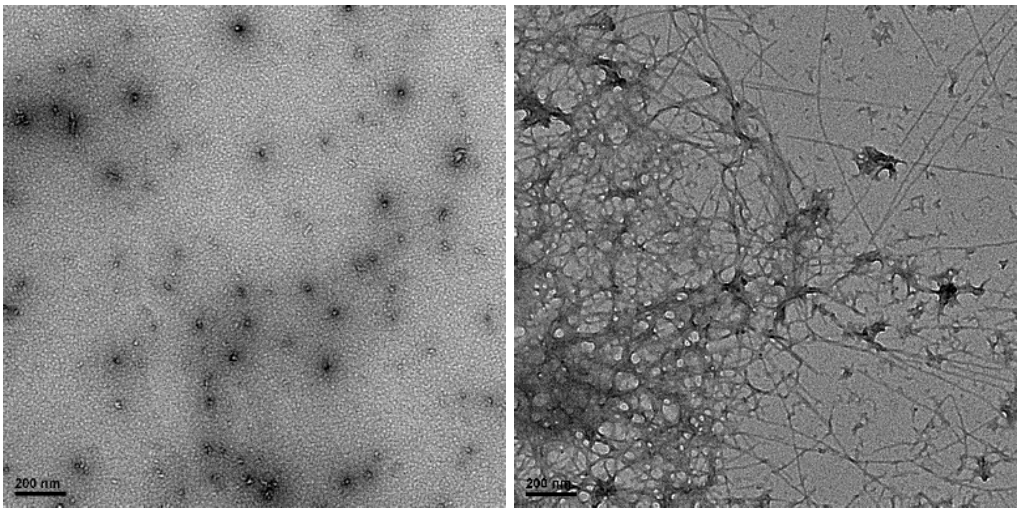

Figure S2. TEM images of $A\beta_{42}$ oligomers (left) and fibrils (right). Scale bar: 200 nm.

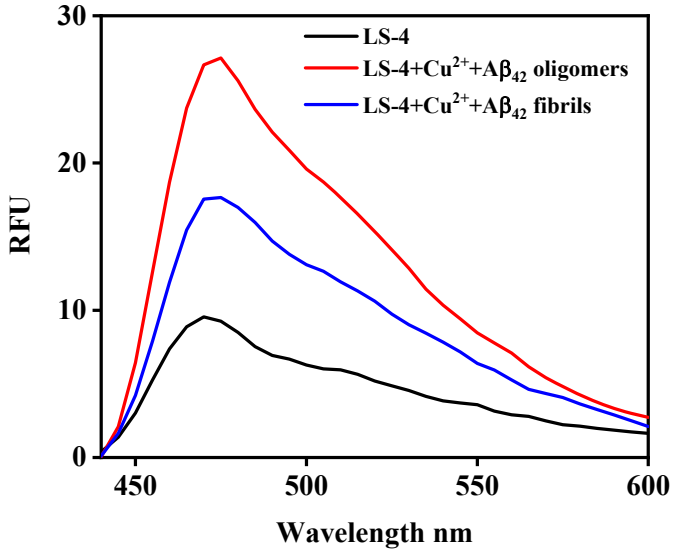

Figure S3. Fluorescence turn-on effect of Cu^{2+}-LS-4 with $A\beta_{42}$ oligomers and fibrils. Cu^{2+}-LS-4 (black), $A\beta_{42}$ oligomer + Pre-LS-4 (red) and $A\beta_{42}$ fibrils + Pre-LS-4 (blue); [$A\beta_{42}$] = 25 μM, [Cu^{2+}-LS-4] = 5 μM, excitation wavelength = 380 nm, PBS pH 7.4 buffer.

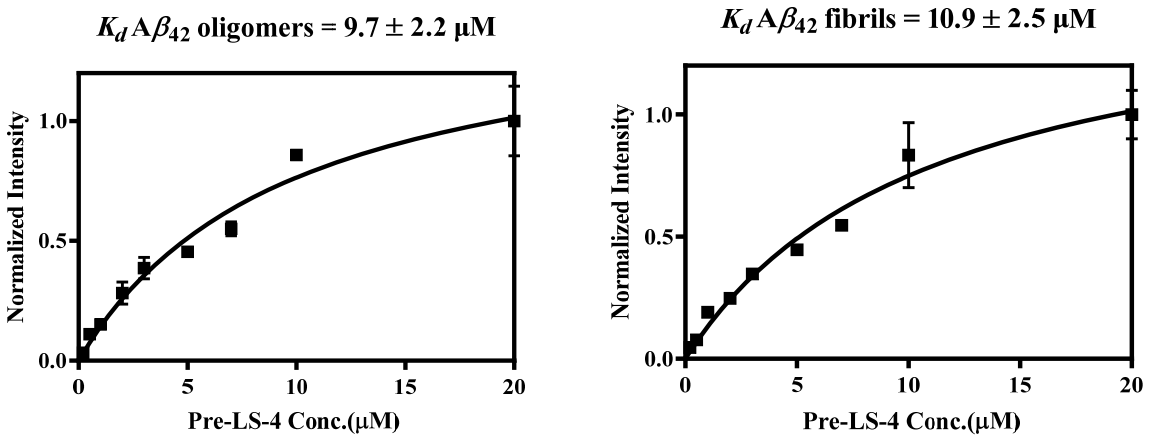

Figure S4. Direct binding constant measurements of Pre-LS-4 with $A\beta_{42}$ oligomers (left) and fibrils (right).

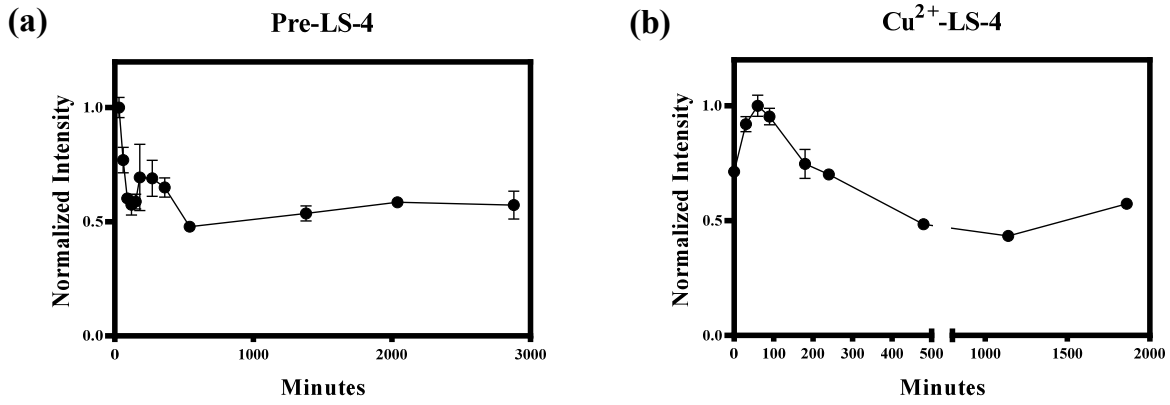

Figure S5. Monitoring of the aggregation process of $A\beta_{42}$ at different time points with (a) Pre-LS-4 and (b) Cu^{2+}-LS-4. The fluorescence intensities of Pre-LS-4 and Cu^{2+}-LS-4 were recorded at 475 nm and 470 nm, respectively. Conditions: [$A\beta_{42}$] = 25 μM, [Pre-LS-4] = [Cu^{2+}-LS-4] = 5 μM. The peptides were incubated in pH = 7.4 PBS buffer at 37 °C with shaking for 48 hours.

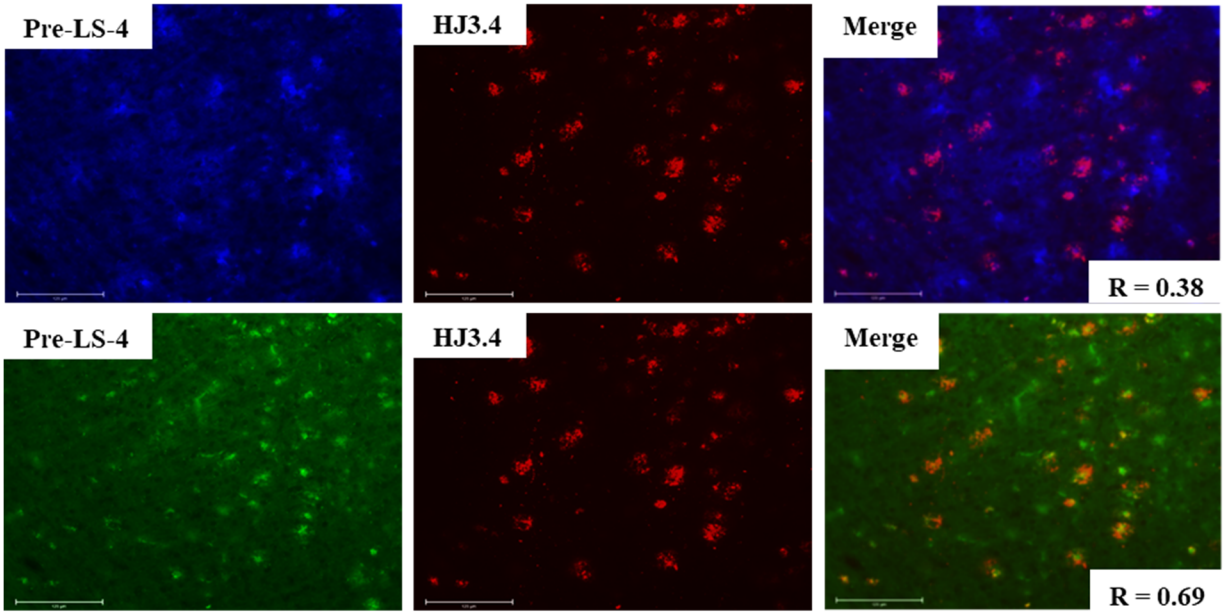

Figure S6. Fluorescence microscopy images of 7-month old 5xFAD mice brain sections co-incubated with compounds Pre-LS-4 (left panels), HJ3.4 (middle panels), and merged images (right panels). Pre-LS-4 was imaged both in the DAPI (top) and FITC (bottom) channels. [Pre-LS-4] = 25 μM, [HJ3.4] = 1 μg/ml. Scale bar = 125 μm.

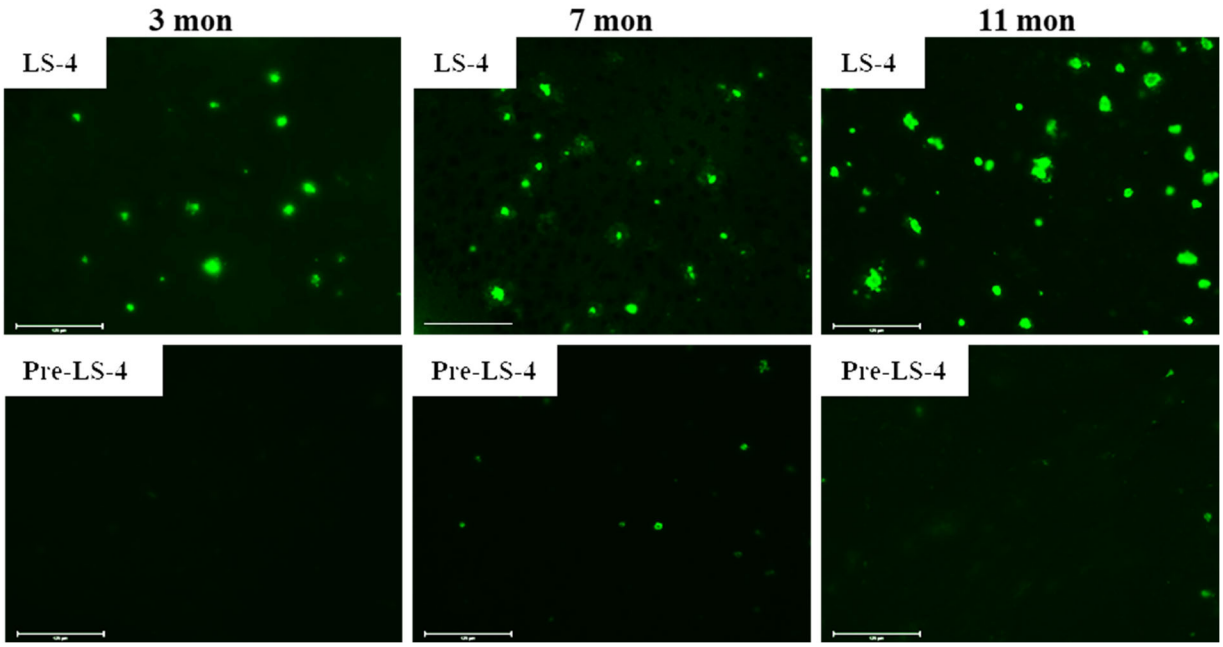

Figure S7. Fluorescence microscopy images of brain sections from 5xFAD mice of different ages, stained with compounds Pre-LS-4 and LS-4. [Pre-LS-4] = [LS-4] = 25 μM. Scale bar = 125 μm.

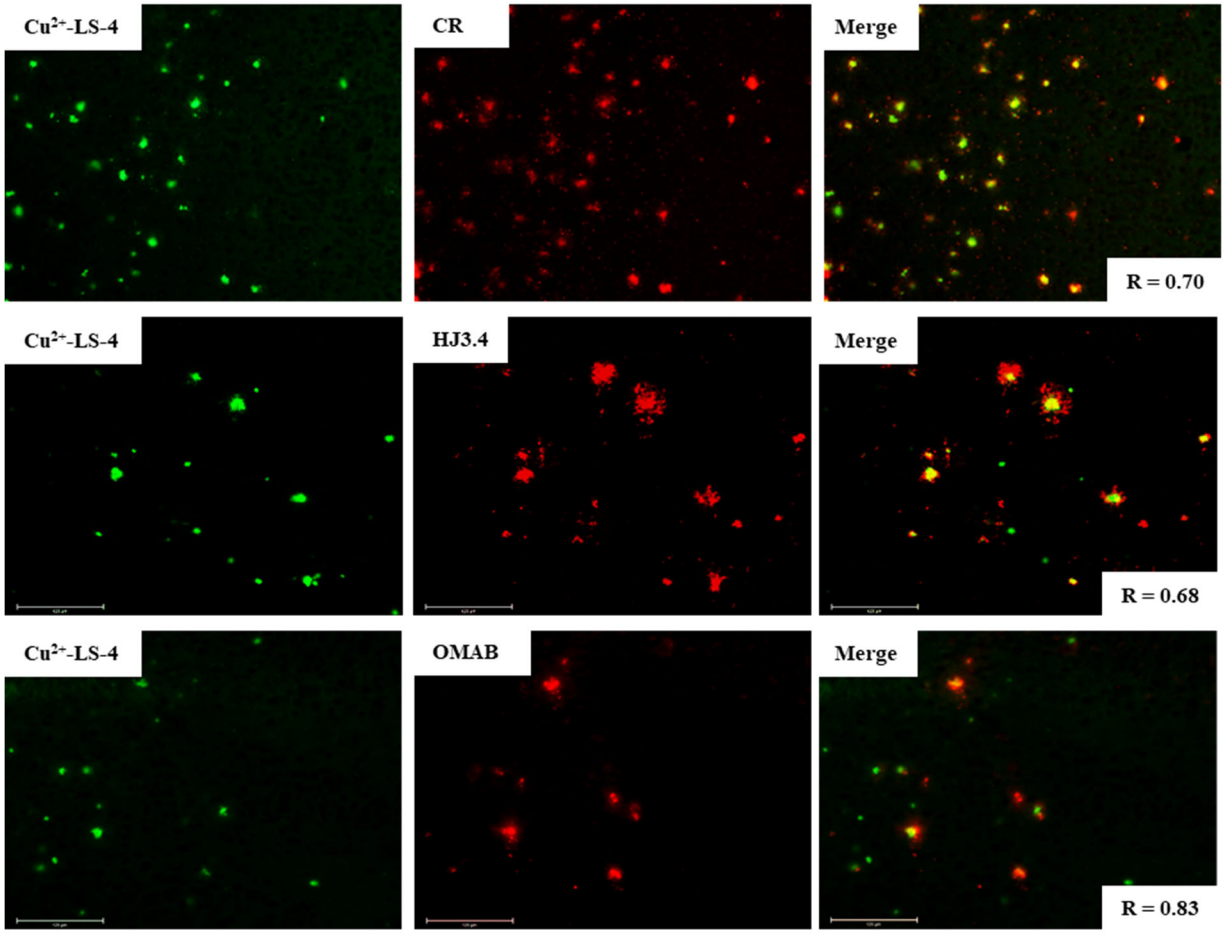

Figure S8. Fluorescence microscopy images of 7-month old 5xFAD mice brain sections incubated with Cu^{2+}-LS-4 complex (left panels), Congo red, HJ3.4, OMAB (middle panels), and merged images (right panels). [Cu^{2+}-LS-4] = 25 μM, [Congo Red] = 5 μM, HJ3.4 = 1 μg/ ml, [OMAB] = 2 μg/ml. Scale bar: 125 μm.

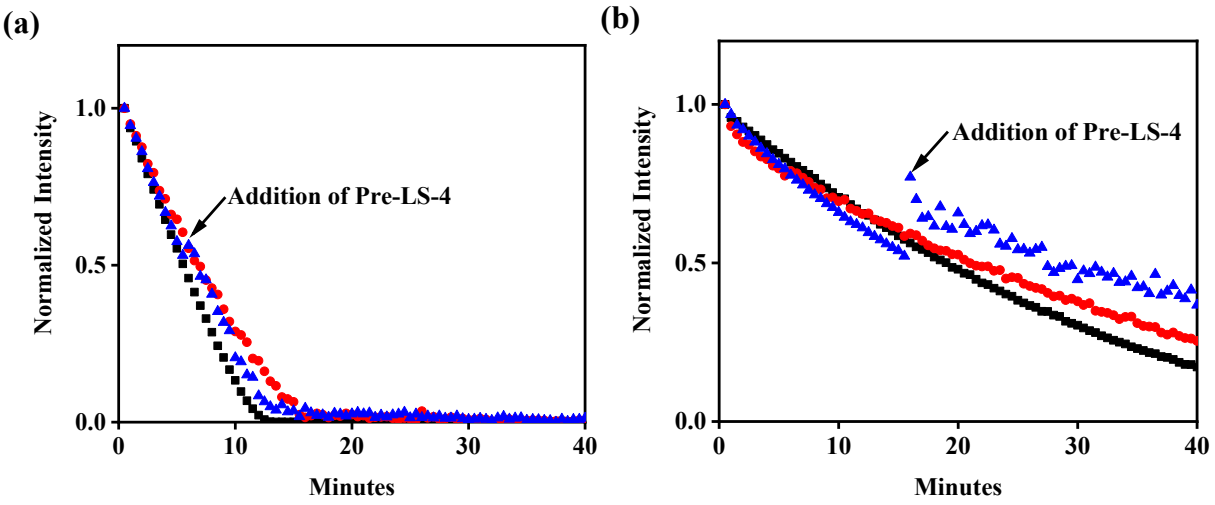

Figure S9. Kinetics of ascorbate consumption monitored by UV-vis spectroscopy at 265 nm. (a) Cu^{2+} + ascorbate (black), Cu^{2+} + Pre-LS-4 + ascorbate (red), Cu^{2+} + ascorbate + Pre-LS-4 (blue); (b) Cu^{2+} + $A\beta_{42}$ + ascorbate (black), Cu^{2+} + $A\beta_{42}$ + Pre-LS-4 + ascorbate (red), Cu^{2+} + $A\beta_{42}$ + ascorbate + Pre-LS-4 (blue). [Cu^{2+}] = 10 μM, [$A\beta_{42}$] = 12 μM, [Pre-LS-4] = 24 μM, [ascorbate] = 100 μM.

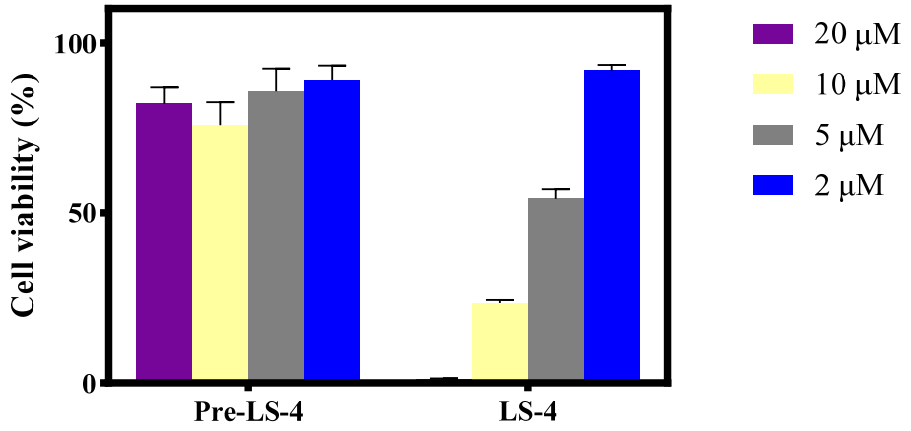

Figure S10. Cytotoxicity of compounds Pre-LS-4 and LS-4 determined by Alamar blue assay. Conditions: [Pre-LS-4] = [LS-4] = 20 µM (purple), 10 µM (yellow), 5 µM (grey), 2 µM (blue). The error bars indicate the standard deviations (n=5).

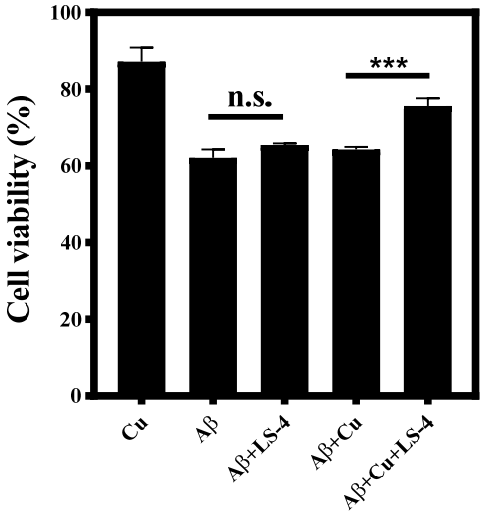

Figure S11. Effects of LS-4 on Cu^{2+}-induced $A\beta_{42}$ cytotoxicity. Conditions: $[A\beta_{42}] = [CuCl_2] =$ 20 μM, [LS-4] = 5 μM. The error bars indicate the standard deviations (n=5), and the statistical analysis was evaluated according to one-way ANOVA (***$p < 0.001$).

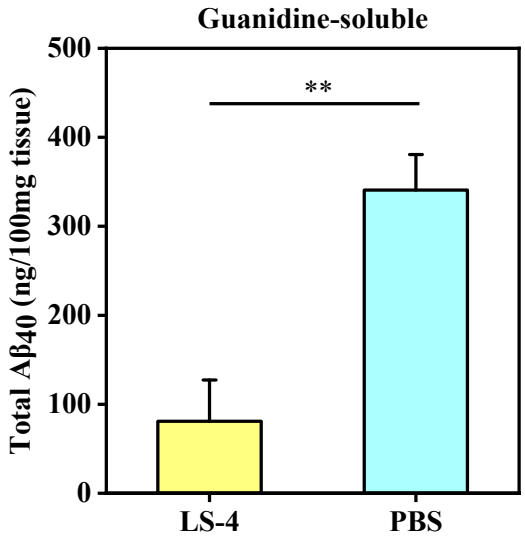

Figure S12. Guanidine-soluble $A\beta_{40}$ levels from AD mouse brain tissues, quantified using ELISA. Error bars represent standard deviations (LS-4 treated mice, n = 5, vehicle-treated mice, n = 3), and the statistical analysis was evaluated according to one-way ANOVA (**$p < 0.01$). Note: the amount of PBS-soluble $A\beta_{40}$ species from the LS-4- and vehicle-treated mice brain homogenates were too low to be detected reproducibly by ELISA.

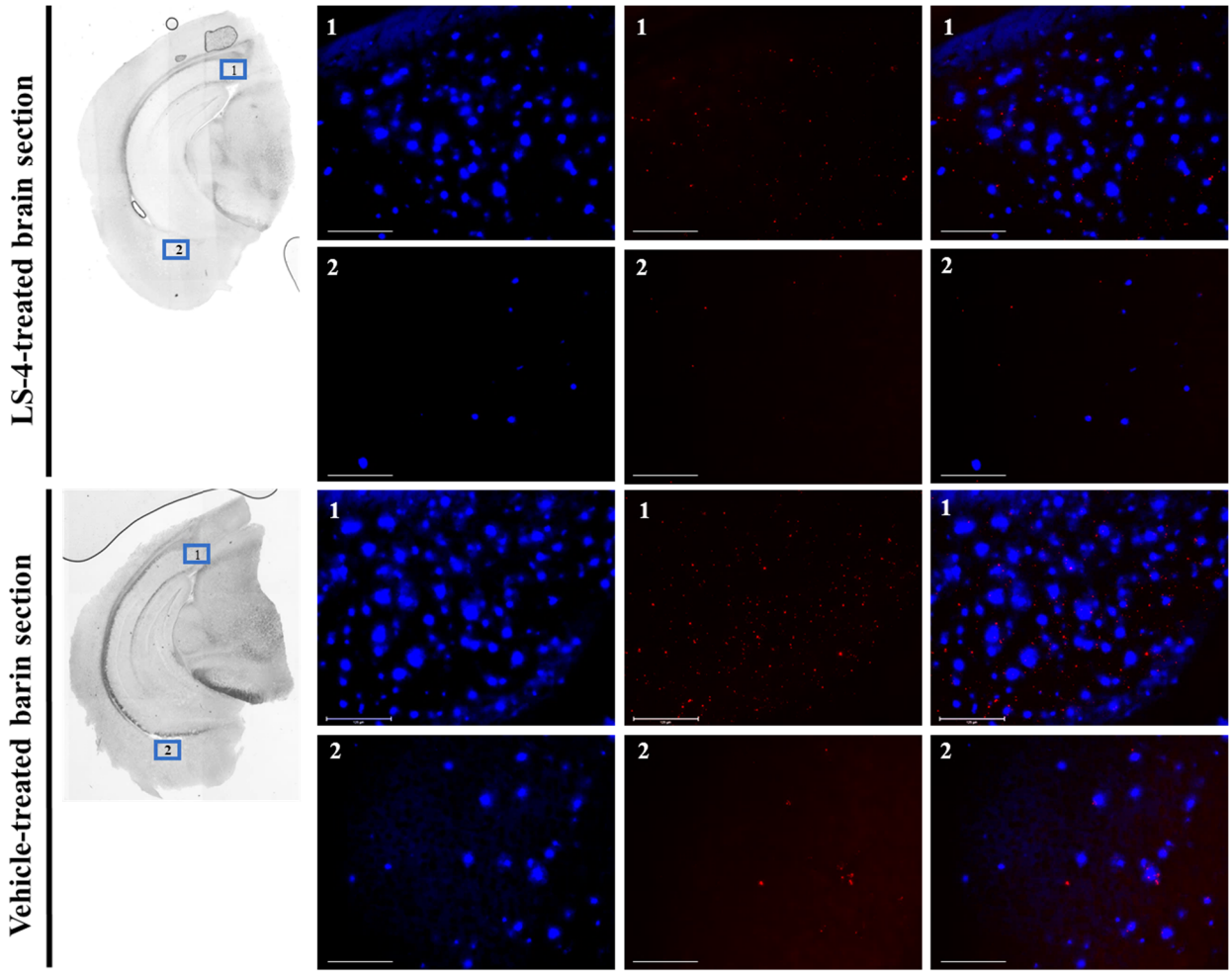

Figure S13. Representative fluorescence images of the CF594-AT8-stained brain sections from 5xFAD mice treated with LS-4 or vehicle. The fluorescence of CF594-AT8 was monitored with a standard Texas Red filter set. All fluorescence images are the maximum intensity projection images obtained from 30 Z-sections collected at 1 μm intervals. Color: red, CF594-AT8 antibody; blue, ThS. Scale bar: 125 μm.

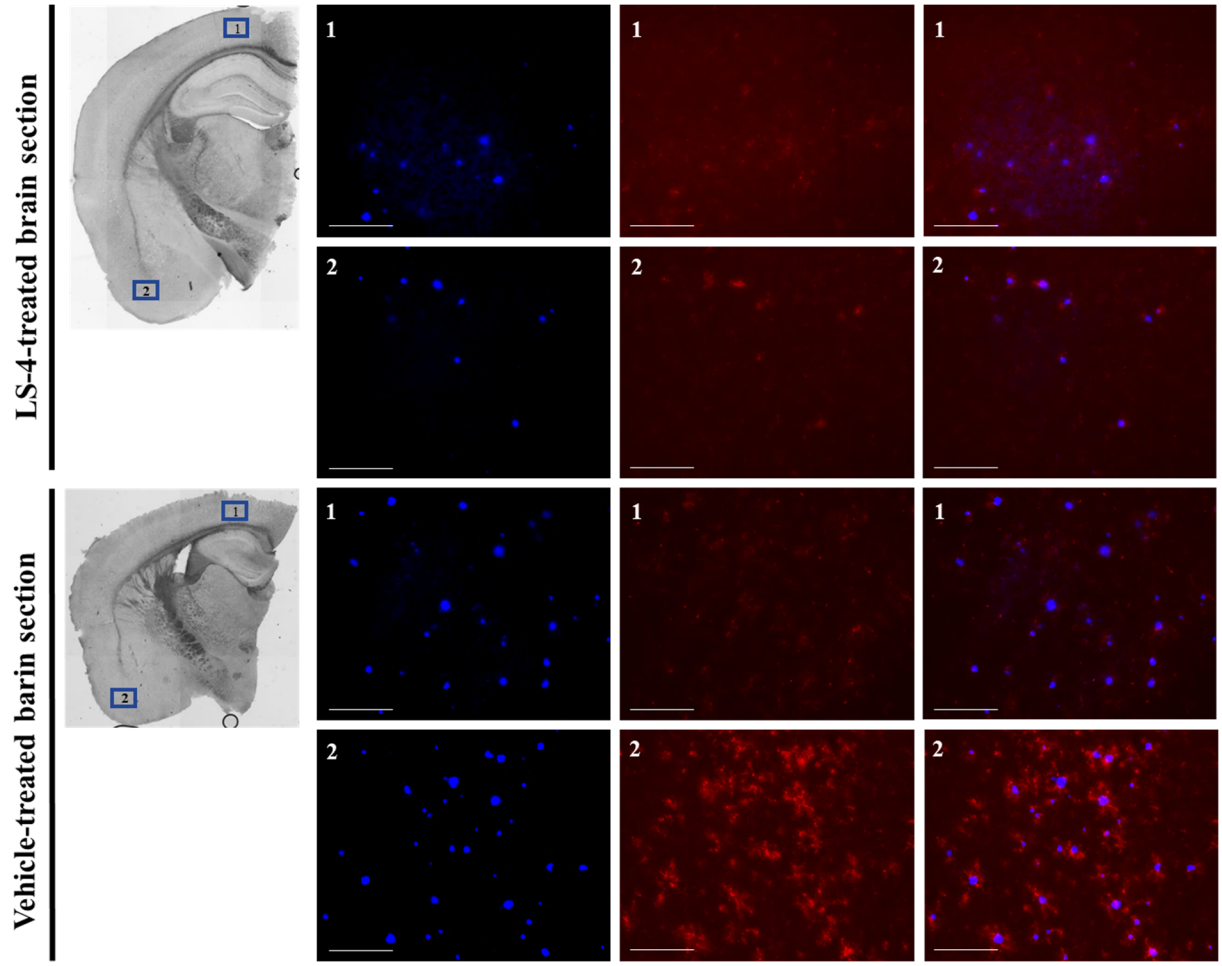

Figure S14. Representative fluorescence images of the CF594-Iba1-stained brain sections from 5xFAD mice treated with LS-4 or vehicle. The fluorescence of CF594-Iba1 was monitored with a standard Texas Red filter set. All fluorescence images are the maximum intensity projection images obtained from 30 Z-sections collected at 1 μm intervals. Color: red, CF594-Iba1 antibody; blue, ThT. Scale bar: 125 μm.

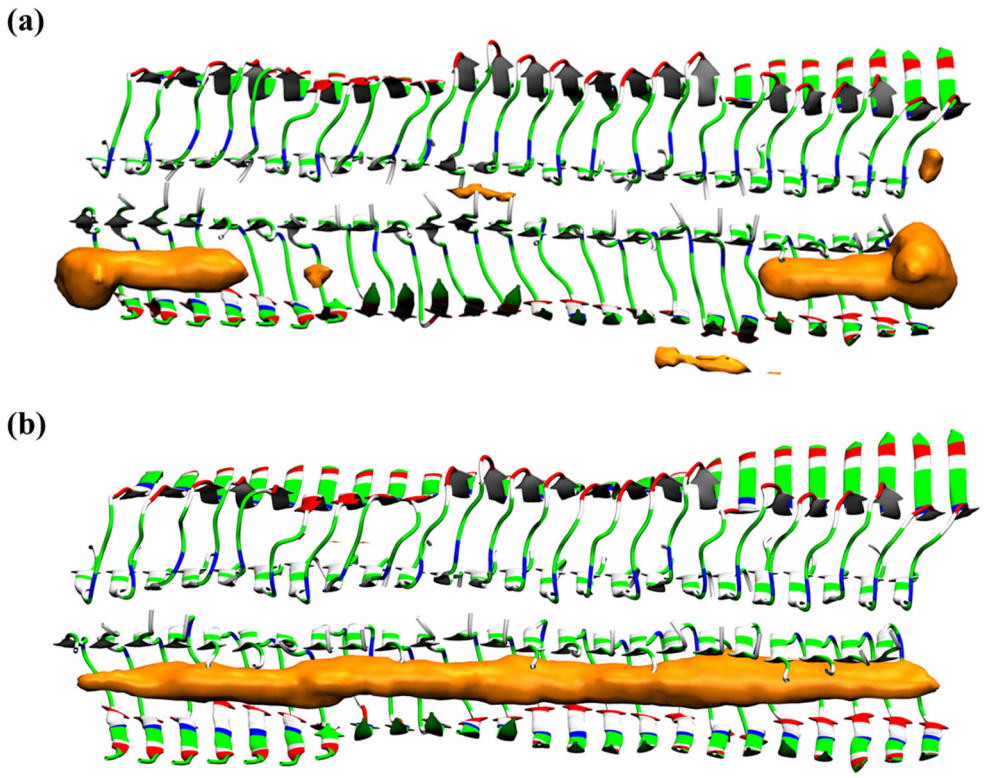

Figure S15. Ensemble docking study performed for LS-4 and Pre-LS-4 onto the Aβ fibril. Proteins are shown in ribbon representation where acidic, basic, polar and nonpolar amino acid residues are shown by red, blue, green and white colors, respectively. Orange surfaces represent a 2% occupancy cutoff of the compounds bound to the protein surface and cavity. (a) Occupancy analysis of LS-4 docked on the Aβ fibril. (b) Occupancy analysis of Pre-LS-4 docked on the Aβ fibril.

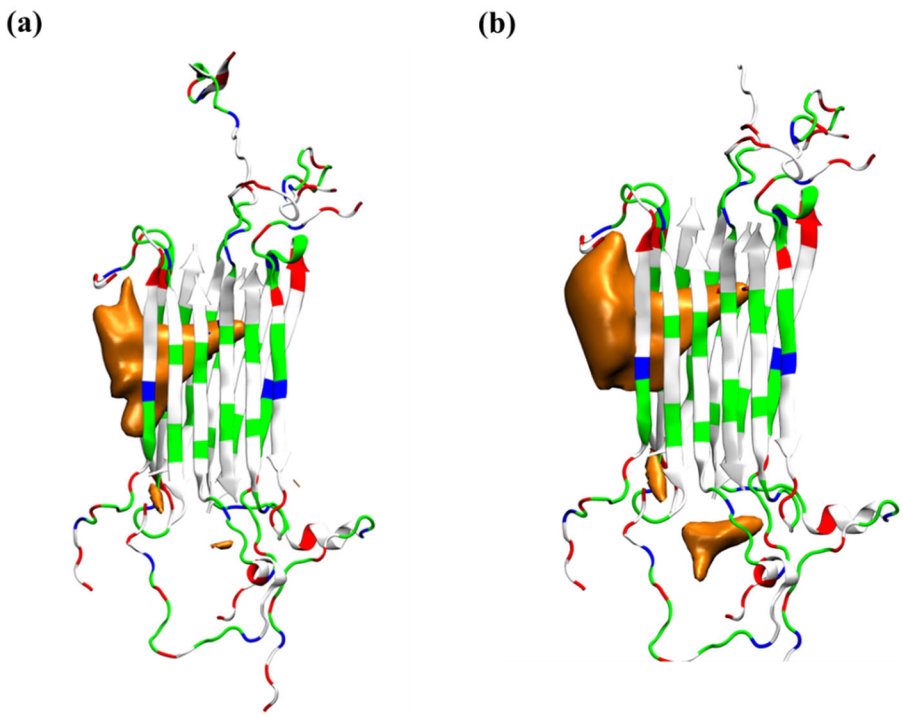

Figure S16. Ensemble docking study performed for LS-4 and Pre-LS-4 onto the Aβ oligomer. Proteins are shown by ribbon representation where acidic, basic, polar and nonpolar amino acid residues are shown by red, blue, green and white colors, respectively. Orange surfaces represent 2% occupancy cutoff of the compounds bound to the protein surface and cavity. (a) Occupancy analysis of LS-4 docked on the Aβ oligomer. (b) Occupancy analysis of Pre-LS-4 docked on the Aβ oligomer.

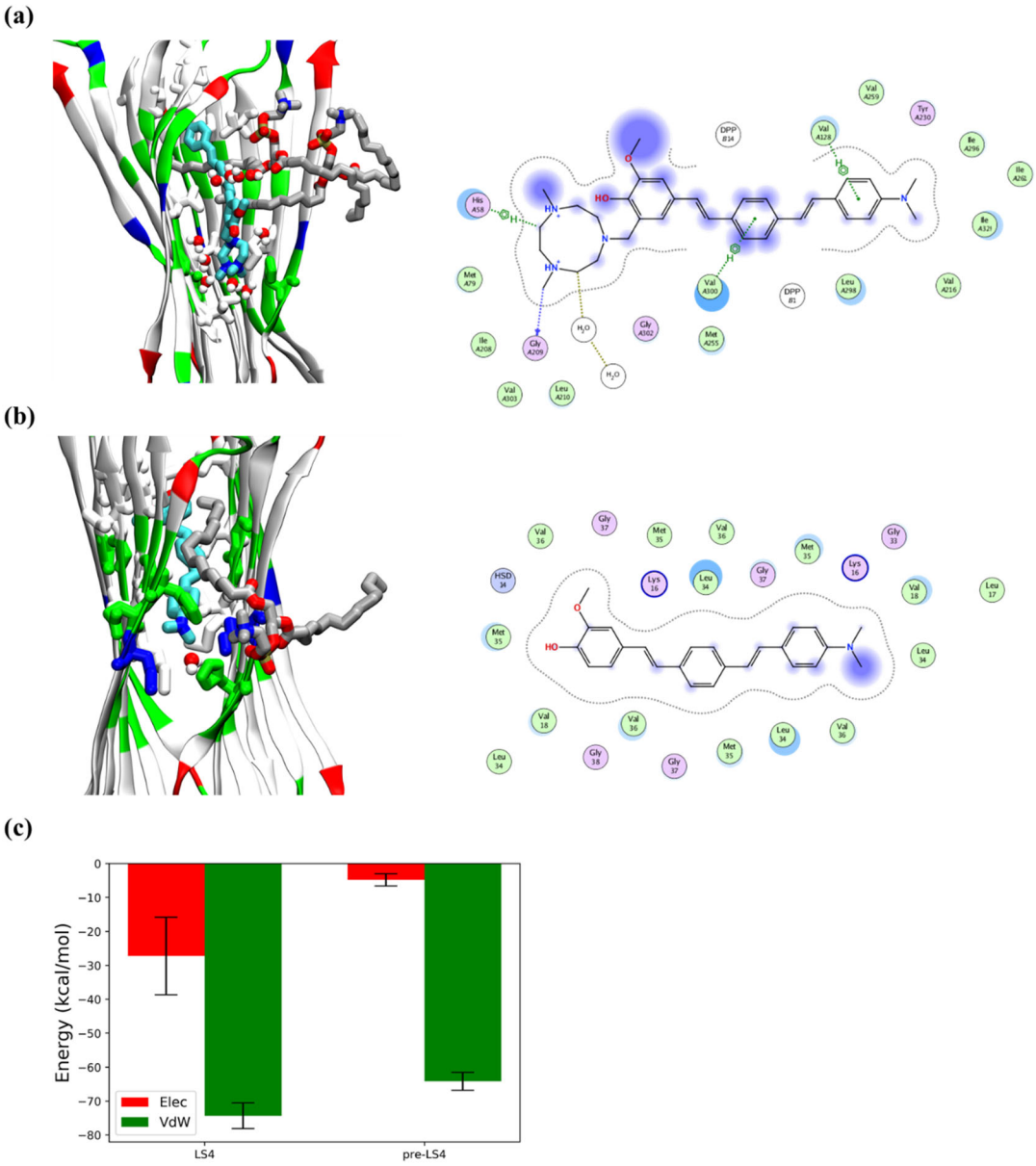

Figure S17. Detailed interactions of LS-4 and Pre-LS-4 docked to the Aβ oligomer embedded in a lipid bilayer after 100 ns simulations are presented. Compounds are shown by licorice representation colored by atoms (C: cyan, N: blue, O: red), the water molecules, lipid molecule and amino acid sidechains within 3 Å of the compounds are displayed by licorice representation. Acidic, basic, polar and nonpolar amino acid residues are shown in red, blue, green and white colors, respectively, water molecules are colored by atoms (O: red, H: white), lipids are also colored by atoms (C: gray, N: blue, O: red, P: yellow). For 2D compound-protein interaction

patterns, the close-by protein residues and solvent molecules are shown in proximity around the compound. The compound is annotated with a proximity contour and solvent exposure while the protein residues are also annotated by solvent exposure. The blue dotted line with arrow is H-bonding with the protein backbone. (a) Interaction of LS-4 with Aβ oligomer. (b) interaction of Pre-LS-4 with Aβ oligomer, (c) electrostatic and van der Waals interaction energies of LS-4 and Pre-LS-4 with Aβ oligomer, averaged over the last 25 ns of the MD simulations.

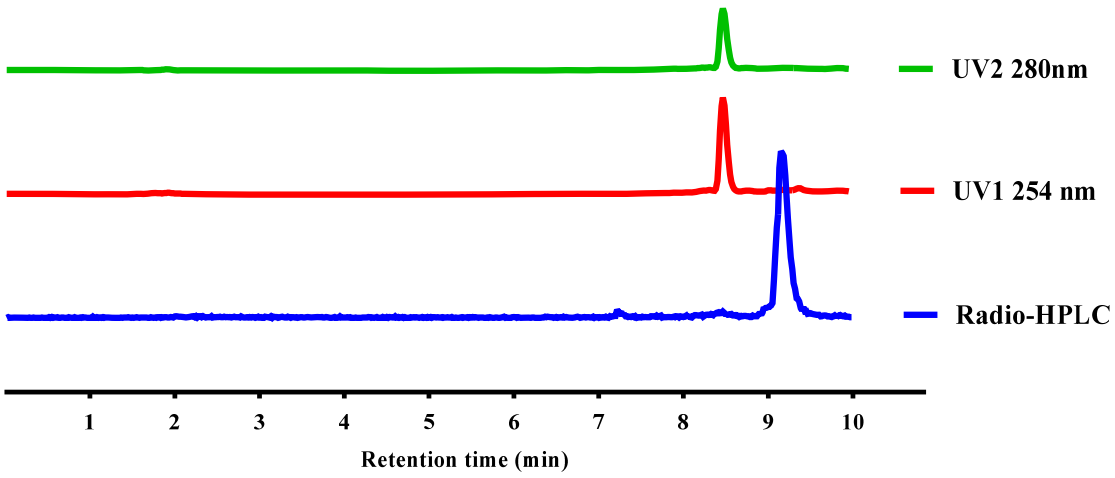

Figure S18. HPLC profiles of LS-4 with dual wavelength 280 nm (green) and 254 nm (red). The retention times were 8.45 min for LS-4. ^{64}Cu-LS-4 (blue) with detection of radioactivity. The retention times were 9.42 min for ^{64}Cu-LS-4, respectively.

Table S1. Overall biodistribution results of ^{64}Cu-LS-4 in AD mice *vs* aged matched WT mice, for the three time points evaluated (2 min, 1, and 4 h; % injected dose per gram, Mean ± SEM).

	AD 2 min	**AD** 1 h	**AD** 4 h	**WT** 2 min	**WT** 1 h	**WT** 4 h
blood	14.76 ± 0.20	5.06 ± 0.27	4.91 ± 0.21	16.19 ± 1.61	4.24 ± 0.20	2.03 ± 0.43
lung	48.31 ± 4.12	17.52 ± 0.41	16.97 ± 1.63	38.34 ± 6.09	13.60 ± 2.91	7.26 ± 3.11
liver	14.65 ± 1.70	18.77 ± 0.90	27.81 ± 0.68	13.23 ± 1.04	15.85 ± 0.89	14.30 ± 1.50
kidney	8.77 ± 0.64	15.20 ± 0.45	30.24 ± 0.42	6.87 ± 0.09	10.64 ± 1.22	11.36 ± 2.44
muscle	0.67 ± 0.06	1.64 ± 0.14	1.79 ± 0.21	0.49 ± 0.02	0.96 ± 0.04	0.75 ± 0.02
brain	**0.79 ± 0.06**	**0.33 ± 0.03**	**0.39 ± 0.02**	**0.75 ± 0.10**	**0.18 ± 0.02**	**0.18 ± 0.00**
bone	1.23 ± 0.13	1.56 ± 0.08	1.80 ± 0.12	0.68 ± 0.06	0.80 ± 0.13	0.66 ± 0.12
tail	11.09 ± 1.15	7.85 ± 0.47	6.73 ± 2.05	5.36 ± 1.83	3.28 ± 1.28	4.00 ± 0.10

[1]H-NMR, [13]C-NMR, and HR-MS spectra of Pre-LS-4

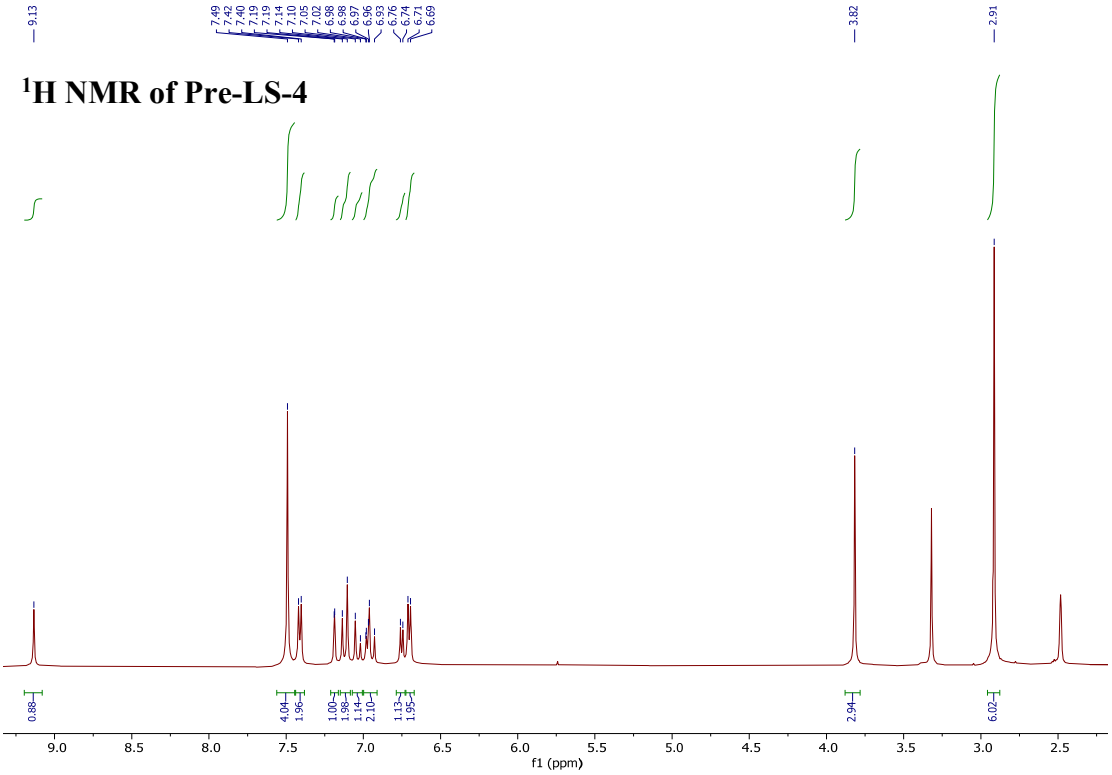

[1]H NMR of Pre-LS-4

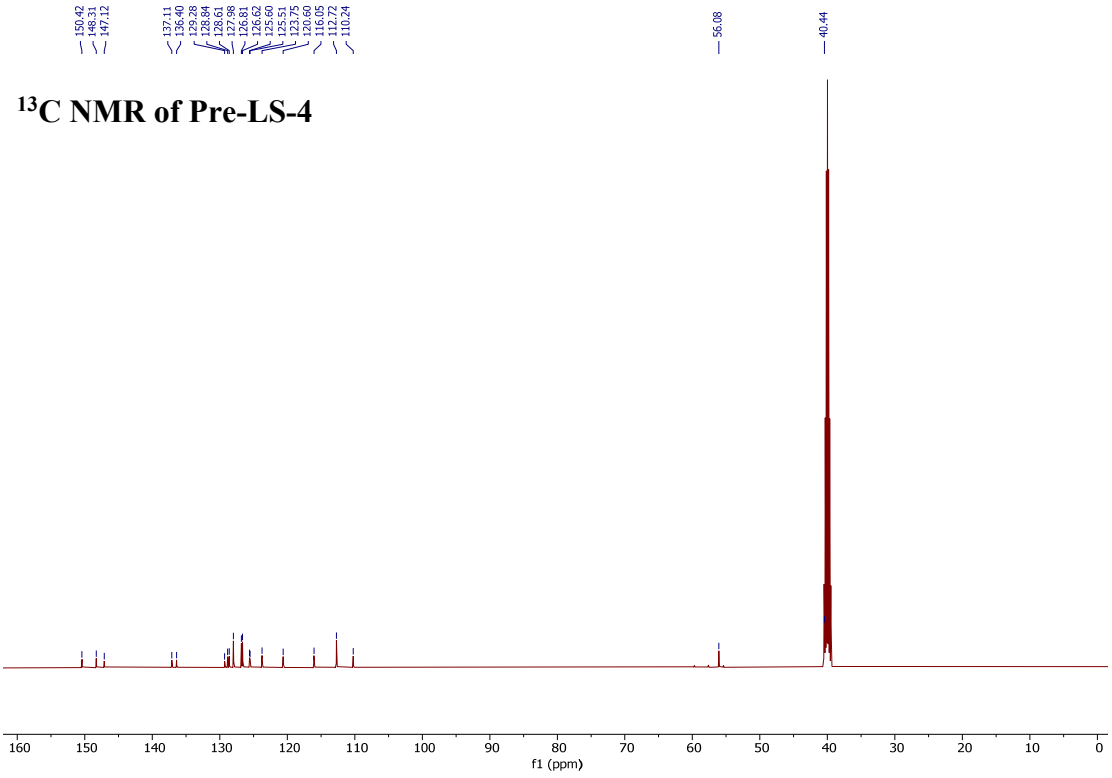

[13]C NMR of Pre-LS-4

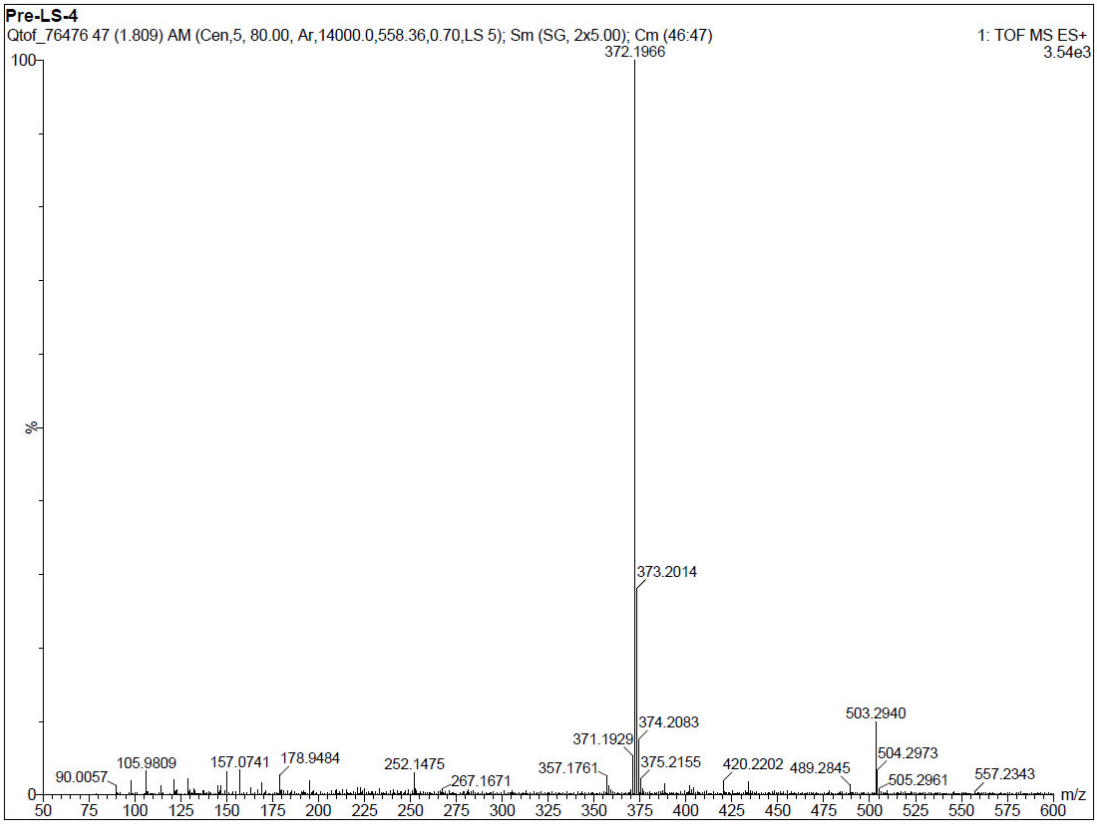
Pre-LS-4
Qtof_76476 47 (1.809) AM (Cen,5, 80.00, Ar,14000.0,558.36,0.70,LS 5); Sm (SG, 2x5.00); Cm (46:47)
1: TOF MS ES+
3.54e3
372.1966
373.2014
374.2083
503.2940
371.1929
504.2973
105.9809
157.0741
178.9484
252.1475
375.2155
420.2202
489.2845
90.0057
267.1671
357.1761
505.2961
557.2343
%
m/z

[1]H-NMR, [13]C-NMR, and HR-MS spectra of LS-4

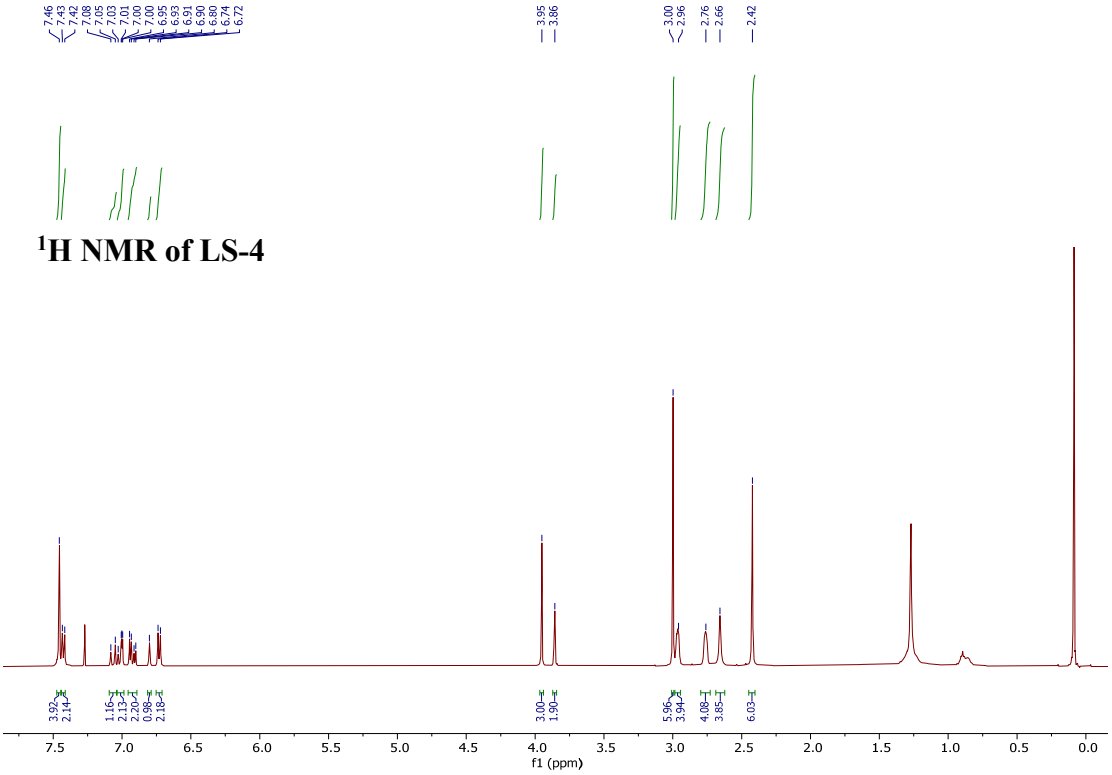

[1]H NMR of LS-4

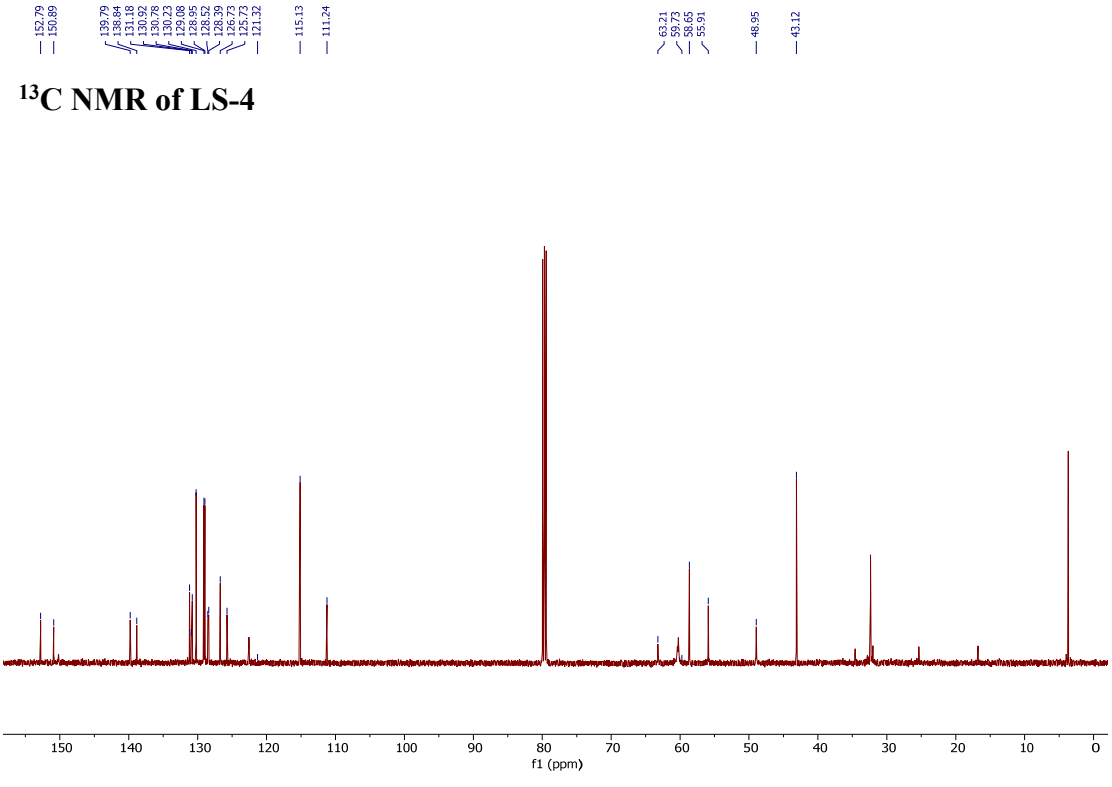

[13]C NMR of LS-4

HR-MS spectra of LS-4

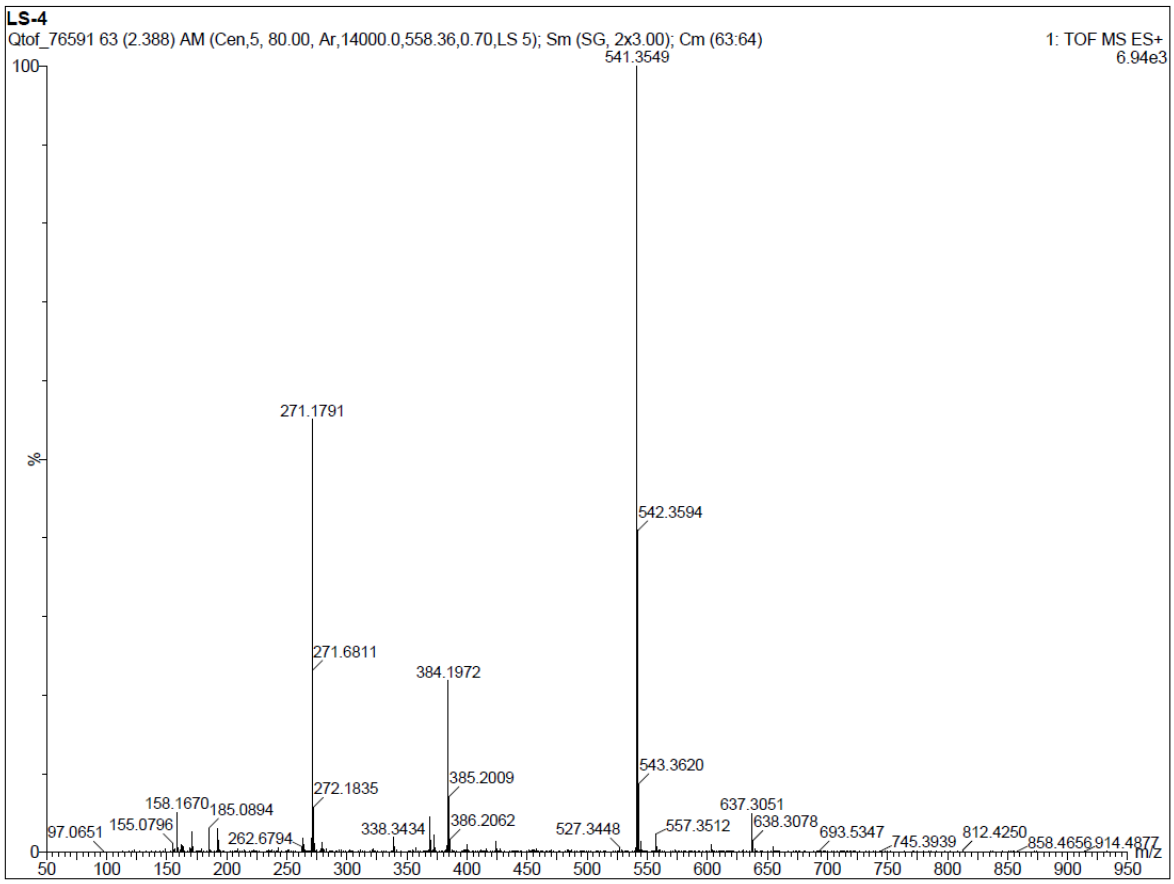

References

1. Yang, J. S.; Lin, Y. D.; Lin, Y. H.; Liao, F. L. Zn(II)-induced ground-state pi-deconjugation and excited-state electron transfer in N,N-bis(2-pyridyl)amino-substituted arenes *J. Org. Chem.* **2004**, *69*, 3517.
2. Zhang, W.; Oya, S.; Kung, M. P.; Hou, C.; Maier, D. L.; Kung, H. F. F-18 Stilbenes as PET imaging agents for detecting beta-amyloid plaques in the brain *J. Med. Chem.* **2005**, *48*, 5980.
3. Jones, M. R.; Mathieu, E.; Dyrager, C.; Faissner, S.; Vaillancourt, Z.; Korshavn, K. J.; Lim, M. H.; Ramamoorthy, A.; Wee Yong, V.; Tsutsui, S.; Stys, P. K.; Storr, T. Multi-target-directed phenol-triazole ligands as therapeutic agents for Alzheimer's disease *Chem. Sci.* **2017**, *8*, 5636.
4. Ran, C. Z.; Xu, X. Y.; Raymond, S. B.; Ferrara, B. J.; Neal, K.; Bacskai, B. J.; Medarova, Z.; Moore, A. Design, Synthesis, and Testing of Difluoroboron-Derivatized Curcumins as Near-Infrared Probes for in Vivo Detection of Amyloid-beta Deposits *J. Am. Chem. Soc.* **2009**, *131*, 15257.
5. Sharma, A. K.; Schultz, J. W.; Prior, J. T.; Rath, N. P.; Mirica, L. M. Coordination Chemistry of Bifunctional Chemical Agents Designed for Applications in ^{64}Cu PET Imaging for Alzheimer's Disease *Inorg. Chem.* **2017**, *56*, 13801.
6. Paravastu, A. K.; Leapman, R. D.; Yau, W. M.; Tycko, R. Molecular structural basis for polymorphism in Alzheimer's beta-amyloid fibrils *Proc. Natl. Acad. Sci. U. S. A.* **2008**, *105*, 18349.
7. Lu, J. X.; Qiang, W.; Yau, W. M.; Schwieters, C. D.; Meredith, S. C.; Tycko, R. Molecular structure of beta-amyloid fibrils in Alzheimer's disease brain tissue *Cell* **2013**, *154*, 1257.
8. Trott, O.; Olson, A. J. Software News and Update AutoDock Vina: Improving the Speed and Accuracy of Docking with a New Scoring Function, Efficient Optimization, and Multithreading *J. Comput. Chem.* **2010**, *31*, 455.
9. Ciudad, S.; Puig, E.; Botzanowski, T.; Meigooni, M.; Arango, A. S.; Do, J.; Mayzel, M.; Bayoumi, M.; Chaignepain, S.; Maglia, G.; Cianferani, S.; Orekhov, V.; Tajkhorshid, E.; Bardiaux, B.; Carulla, N. Abeta(1-42) tetramer and octamer structures reveal edge conductivity pores as a mechanism for membrane damage *Nat. Commun.* **2020**, *11*, 3014.
10. Phillips, J. C.; Braun, R.; Wang, W.; Gumbart, J.; Tajkhorshid, E.; Villa, E.; Chipot, C.; Skeel, R. D.; Kale, L.; Schulten, K. Scalable molecular dynamics with NAMD *J. Comput. Chem.* **2005**, *26*, 1781.
11. Phillips, J. C.; Hardy, D. J.; Maia, J. D. C.; Stone, J. E.; Ribeiro, J. V.; Bernardi, R. C.; Buch, R.; Fiorin, G.; Henin, J.; Jiang, W.; McGreevy, R.; Melo, M. C. R.; Radak, B. K.; Skeel, R. D.; Singharoy, A.; Wang, Y.; Roux, B.; Aksimentiev, A.; Luthey-Schulten, Z.; Kale, L. V.; Schulten, K.; Chipot, C.; Tajkhorshid, E. Scalable molecular dynamics on CPU and GPU architectures with NAMD *J. Chem. Phys.* **2020**, *153*, 044130.

12. Huang, J.; Rauscher, S.; Nawrocki, G.; Ran, T.; Feig, M.; de Groot, B. L.; Grubmuller, H.; MacKerell, A. D. CHARMM36m: an improved force field for folded and intrinsically disordered proteins *Nat. Methods* **2017**, *14*, 71.
13. Klauda, J. B.; Venable, R. M.; Freites, J. A.; O'Connor, J. W.; Tobias, D. J.; Mondragon-Ramirez, C.; Vorobyov, I.; MacKerell, A. D.; Pastor, R. W. Update of the CHARMM All-Atom Additive Force Field for Lipids: Validation on Six Lipid Types *J. Phys. Chem. B* **2010**, *114*, 7830.
14. Brooks, B. R.; Brooks, C. L.; Mackerell, A. D.; Nilsson, L.; Petrella, R. J.; Roux, B.; Won, Y.; Archontis, G.; Bartels, C.; Boresch, S.; Caflisch, A.; Caves, L.; Cui, Q.; Dinner, A. R.; Feig, M.; Fischer, S.; Gao, J.; Hodoscek, M.; Im, W.; Kuczera, K.; Lazaridis, T.; Ma, J.; Ovchinnikov, V.; Paci, E.; Pastor, R. W.; Post, C. B.; Pu, J. Z.; Schaefer, M.; Tidor, B.; Venable, R. M.; Woodcock, H. L.; Wu, X.; Yang, W.; York, D. M.; Karplus, M. CHARMM: The Biomolecular Simulation Program *J. Comput. Chem.* **2009**, *30*, 1545.
15. Jorgensen, W. L.; Chandrasekhar, J.; Madura, J. D.; Impey, R. W.; Klein, M. L. Comparison of Simple Potential Functions for Simulating Liquid Water *J. Chem. Phys.* **1983**, *79*, 926.
16. Martyna, G. J.; Tobias, D. J.; Klein, M. L. Constant-Pressure Molecular-Dynamics Algorithms *J. Chem. Phys.* **1994**, *101*, 4177.
17. Ryckaert, J. P.; Ciccotti, G.; Berendsen, H. J. C. Numerical-Integration of Cartesian Equations of Motion of a System with Constraints - Molecular-Dynamics of N-Alkanes *J. Comput. Phys.* **1977**, *23*, 327.
18. Darden, T.; York, D.; Pedersen, L. Particle Mesh Ewald - an N.Log(N) Method for Ewald Sums in Large Systems *J. Chem. Phys.* **1993**, *98*, 10089.
19. Humphrey, W.; Dalke, A.; Schulten, K. VMD: Visual molecular dynamics *J. Mol. Graphics Modell.* **1996**, *14*, 33.
20. Kume, M.; Carey, P. C.; Gaehle, G.; Madrid, E.; Voller, T.; Margenau, W.; Welch, M. J.; Lapi, S. E. A semi-automated system for the routine production of copper-64 *Appl. Radiat. Isot.* **2012**, *70*, 1803.
21. Han, B. H.; Zhou, M. L.; Abousaleh, F.; Brendza, R. P.; Dietrich, H. H.; Koenigsknecht-Talboo, J.; Cirrito, J. R.; Milner, E.; Holtzman, D. M.; Zipfel, G. J. Cerebrovascular Dysfunction in Amyloid Precursor Protein Transgenic Mice: Contribution of Soluble and Insoluble Amyloid-beta Peptide, Partial Restoration via gamma-Secretase Inhibition *J. Neurosci.* **2008**, *28*, 13542.